Available online at www.sciencedirect.com

ScienceDirect

Proceedings of the Combustion Institute 37 (2019) 1623–1630

Proceedings of the Combustion Institute

www.elsevier.com/locate/proci

Effects of fuel stratification on ignition kernel development and minimum ignition energy of n-decane/air mixtures

Yuan Wang, Wang Han, Zheng Chen*

State Key Laboratory for Turbulence and Complex Systems (SKLTCS), Department of Mechanics and Engineering Science, College of Engineering, Peking University, Beijing 100871, China

Received 8 November 2017; accepted 18 May 2018
Available online 21 June 2018

Abstract

Fuel-stratified combustion has broad application due to its promising advantages in extension of lean flammability limit, improvement of flame stabilization, enhancement of lean combustion, etc. In the literature, there are many studies on flame propagation in fuel-stratified mixtures. However, there is little attention on ignition in fuel-stratified mixtures. In this study, one-dimensional numerical simulation is conducted to investigate the ignition and spherical flame kernel propagation in fuel-stratified n-decane/air mixtures. The emphasis is placed on assessing the effects of fuel stratification on the ignition kernel propagation and critical ignition condition. First, ignition and flame kernel propagation in homogeneous n-decane/air mixture are studied and different flame regimes are identified. The minimum ignition energy (MIE) of the homogeneous n-decane/air mixture is obtained and it is found to be very sensitive to the equivalence ratio under fuel-lean conditions. Then, ignition and flame kernel propagation in fuel-stratified n-decane/air mixture are investigated. The inner equivalence ratio and stratification radius are found to have great impact on ignition kernel propagation. The MIEs at different fuel-stratification conditions are calculated. The results indicate that for fuel-lean n-decane/air mixture, fuel stratification can greatly promote ignition and reduce the MIE. Six distinct flame regimes are observed for successful ignition in fuel-stratified mixture. It is shown that the ignition kernel propagation can be induced by not only the ignition energy deposition but also the fuel-stratification. Moreover, it is found that to achieve effective ignition enhancement though fuel stratification, one needs properly choose the values of stratification radius and inner equivalence ratio.

Keywords: Fuel stratification; Ignition; Spherical flame propagation; N-decane/air

1. Introduction

Fuel-stratified combustion occurs in many practical combustion facilities such as internal combustion engines, gas turbine engines and industrial furnaces. In these facilities, perfectly homogeneous

* Corresponding author.
E-mail address: cz@pku.edu.cn (Z. Chen).

https://doi.org/10.1016/j.proci.2018.05.087
1540-7489

mixing of the reactants cannot be achieved and non-uniform spatial distribution of equivalence ratio always exists. Compared to homogeneous premixed combustion, fuel-stratified combustion has several advantages. For examples, fuel-stratified combustion can improve flame stability and enhance combustion under very fuel lean conditions [1]; fuel stratification in direct-injection spark-ignition (DISI) engines helps to extend the lean limit of engine operation [2]; and fuel stratification can be used to control combustion phasing in HCCI engines [3] and to prevent knocking in DISI engines [4]. Despite its wide application, fundamental understanding of stratified combustion is still incomplete compared to homogeneous premixed combustion.

In the literature, there are many studies on premixed flame propagation in fuel-stratified mixtures (e.g., [5–13]). For examples, Ra [5] measured and simulated spherical flame propagation in a rich-to-lean stratified methane/air mixture and found that stratified flame has a memory of previous flame history. Da Cruz et al. [6] demonstrated the memory effects of stratified combustion. Kang and Kyritsis [7] designed a burner to study flame propagation speed in compositionally stratified methane/air mixture. They observed that flame speed increase in the vicinity of the flammability limits and for high equivalence ratio gradients. They [8] also conducted theoretical analysis on this observation. Zhou and Hochgreb [9] found that stratification has stronger influence on counterflow flame behavior at higher strain rate. Balusamy et al. [10] used simultaneous PIV-PLIF techniques to measure the flame propagation initiated from a richer mixture and propagating into a lean homogeneous mixture. Zhang and Abraham [11] assessed the effects of species diffusion on stratified flame speed. Patel and Chakraborty [12,13] conducted 3D DNS with one-step chemistry for the forced ignition in stratified mixtures and found that the initial equivalence ratio distribution greatly affects the combustion process. All these studies indicated that flame propagation in fuel-stratified mixture has different characteristics compared to that in homogeneous mixture.

Ignition and flame propagation are two fundamental combustion processes. Most of previous studies on fuel-stratified combustion [5–13] focused on flame propagation, while there is little attention on ignition. The characteristics of ignition kernel propagation in fuel-stratified mixtures are not well understood. This motivates the present work, which investigates the ignition and flame kernel propagation in fuel-stratified mixtures. To the authors' knowledge, the only work on ignition kernel development in fuel-stratified mixture was conducted by Ra [5], Balusamy et al. [10], and Patel and Chakraborty [12,13] as mentioned above. However, these studies [5,10,12,13] did not investigate the influence of fuel stratification on the critical ignition condition and small ignition kernel evolution, which shall be assessed in the present work.

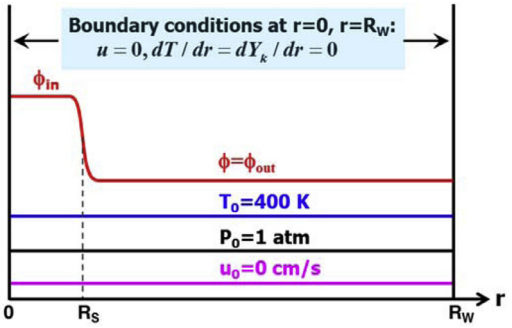

Fig. 1. Schematic of the initial and boundary conditions used in the simulation of ignition and spherical flame kernel propagation in fuel-stratified n-decane/air mixture.

It is well known that successful ignition can be achieved only when the ignition energy is higher than the so-called minimum ignition energy (MIE) [14]. For ignition in fuel-lean mixtures, fuel supplement to the reaction zone through mass diffusion determines the ignition kernel propagation [15,16]. Therefore for fuel-lean mixture, fuel stratification with higher equivalence ratio at the ignition kernel than that in the surroundings is expected to enhance ignition kernel propagation and thereby promote ignition.

In this study, one-dimensional numerical simulation considering detailed chemistry and transport is conducted to investigate ignition in n-decane/air mixtures. The objective is to assess the effects of fuel stratification on the ignition kernel propagation and on the MIE. Since n-decane is one of the main components of surrogate jet fuel and it is difficult to ignite fuel-lean n-decane/air mixture, especially high altitude conditions, n-decane is chosen for the current study.

2. Numerical model and methods

We consider spherical ignition kernel propagation in fuel-stratified n-decane/air mixture. Stratified mixture is ignited in the center and the resulting spherical flame kernel propagates outwardly. Spherical symmetry is assumed and thereby one-dimensional simulation is conducted. The initial and boundary conditions are sketched in Fig. 1. Fuel stratification is introduced by specifying a gradual change in the initial equivalence ratio profile using the hyperbolic tangent function:

$$\phi(r, t{=}0) = \frac{\phi_{in} + \phi_{out}}{2} - \frac{\phi_{in} - \phi_{out}}{2} \tanh\left(\frac{r - R_S}{\delta}\right) \quad (1)$$

where ϕ_{in} and ϕ_{out} are respectively the inner and outer equivalence ratio; R_S is the stratification radius; and δ represents the mixing layer thickness. The initial mixture is homogeneous if $\phi_{in} = \phi_{out}$. As shown in the Supplementary Document, the value δ has little influence on flame propagation speed. Therefore, in all simulations we fix $\delta = 0.04$ mm. Fuel stratification is characterized only by three parameters, ϕ_{in}, ϕ_{out} and R_S. As shown in Fig. 1, the initial temperature of $T_0 = 400$ K, pressure of $P_0 = 1$ atm, and flow velocity of $u_0 = 0$ cm/s are uniformly distributed in the whole computational domain of $0 \le r \le R_W$. The initial temperature of 400 K was chosen only to ensure n-decane is gaseous. The chamber radius is fixed to be $R_W = 20$ cm and only flames with radii below 2 cm are considered.

The ignition kernel propagation is simulated using the in-house code A-SURF [17–19]. The CHEMKIN packages are included in A-SURF to calculate chemical reaction rates. The chemical mechanism for n-decane oxidation includes 54 species and 382 elementary reactions. It was developed by Dryer and coworkers [20,21] and was used by Kim et al. [22]. We did not try one-step chemistry model since previous work [22] showed that the chemistry model has strong impact on the prediction of the ignition kernel development. Adaptive mesh is used and the propagating reaction front is always fully covered by the finest mesh with the size of 7.8 μm. As shown in the Supplementary Document, grid convergence has been ensured. A-SURF has been successfully used in previous studies on ignition and flame propagation [17–19,22–24]. Details on governing equations and numerical schemes of A-SURF are in Refs. [17–19].

To mimic the practical spark ignition process in which energy is deposited around the center during a short period, the following source term is included in the energy equation [24]:

$$q_{ig}(r,t) = \begin{cases} \dfrac{E}{\pi^{1.5} r_{ig}^3 \tau_{ig}} \exp\left[-\left(\dfrac{r}{r_{ig}}\right)^2\right] & if\ t < \tau_{ig} \\ 0 & if\ t \ge \tau_{ig} \end{cases} \quad (2)$$

where E is the total ignition energy deposited into the mixture; τ_{ig} the duration of energy deposition; and r_{ig} the ignition kernel radius. The MIE is calculated by trial-and-error with relative error below 2%. It is noted that the MIE is affected by both r_{ig} and τ_{ig} [14,25]. Since the objective of this study is to assess the effects of fuel-stratification on ignition and flame kernel propagation, the duration of ignition energy deposition and the ignition kernel radius are both kept constant with $\tau_{ig} = 0.5$ ms and $r_{ig} = 0.5$ mm, respectively. The main conclusions are independent of the values of τ_{ig} and r_{ig}. The $\tau_{ig} = 0.5$ ms was chosen to ensure that lean mixture with $\phi = 0.7$ can be successfully ignited. We used the same $r_{ig} = 0.5$ mm for all cases so that we can compare the MIEs of different stratification. In addition, the simulations with different values of τ_{ig} and r_{ig} are also performed and shown in the Supplementary Document.

It is noted that the simplified ignition model used in our simulation is different from practical spark ignition in engines. Therefore, quantitative comparisons of MIEs between simulations and experiments are difficult. However, the simplified model helps to get fundamental understanding of forced ignition in fuel-stratified mixture. This study constitutes a first step towards understanding stratified forced ignition in practice.

3. Results and discussion

3.1. Homogeneous mixture

We first consider ignition and spherical flame kernel propagation in homogeneous mixture (i.e., $\phi_{in} = \phi_{out}$).

Figure 2 shows the effects of ignition energy, E, on the evolution of flame propagation speed, S_b, for lean ($\phi = 0.8$) $nC_{10}H_{22}$/air. In simulation, the flame radius, R_f, is defined as the position of maximum heat release rate; and $S_b = dR_f/dt$. The MIE for this mixture is $E_{min} = 1.8$ mJ. Flame initiation fails for $E = 1.75$ mJ $< E_{min}$ (line #1 in Fig. 2). Only for $E > E_{min}$ can a self-sustained propagating spherical flame be successfully initiated (lines #2–4 in Fig. 2). Similar to previous studies [22,26], Fig. 2 indicates that there exist four distinct flame regimes for $E = 1.85$ mJ (line #2 in Fig. 2): the ignition energy induced flame kernel propagation regime (I), the unsteady flame transition regime (II), the overdriven flame propagation regime (III), and the normal flame propagation regime (IV). Regimes I to IV corresponds to AB, BC, CD and DE in

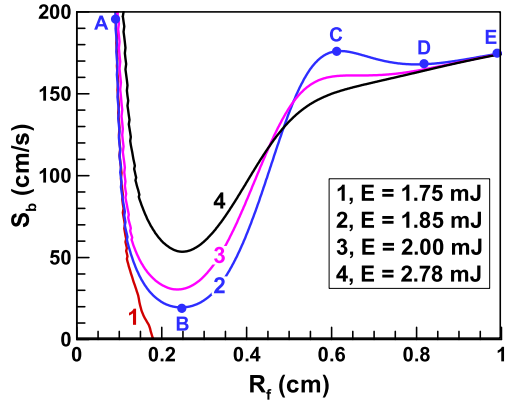

Fig. 2. Change of the flame propagation speed with flame radius for homogeneous $nC_{10}H_{22}$/air with $\phi = 0.8$ and different ignition energies.

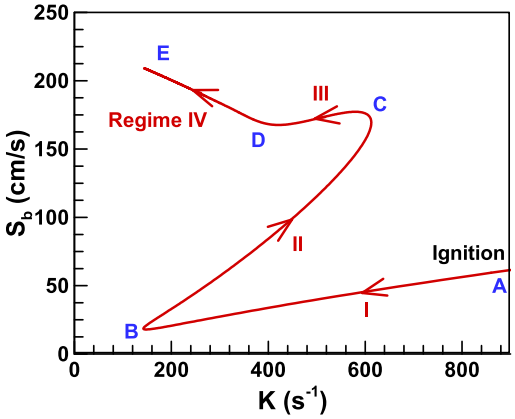

Fig. 3. Change of the flame propagation speed with stretch rate for homogeneous $nC_{10}H_{22}$/air with $\phi = 0.8$ and $E = 1.85$ mJ (same as line #2 in Fig. 2). The arrow indicates flame propagation direction (i.e., increase in flame radius).

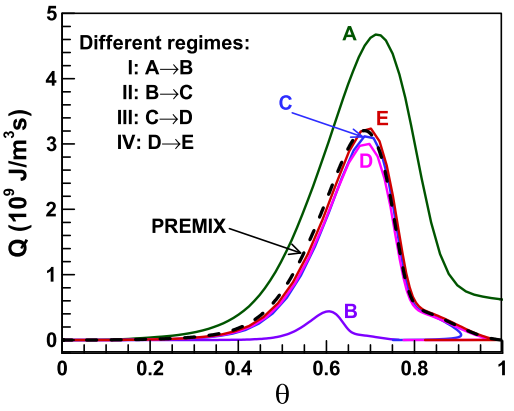

Fig. 4. Change of the heat release rate with normalized temperature for homogeneous $nC_{10}H_{22}$/air with $\phi = 0.8$ and $E = 1.85$ mJ. The dashed line corresponds to the PREMIX results for adiabatic planar flame. Points A-E correspond to those in Figs. 2 and 3.

Fig. 2, respectively. These four regimes are more clearly demonstrated in Fig. 3, which plots S_b as a function of stretch rate, K, which is defined as $K = 2S_b/R_f$.

In regime I, the ignition kernel propagation is mainly driven by ignition energy deposited around the center. Therefore, the ignition kernel propagation speed decreases quickly along AB in Fig. 2. Before the ignition kernel reaches point A, it has very high speed due to the excess enthalpy from the initial external energy addition. At point B with $R_f = 0.25$ cm, the ignition kernel has the lowest propagation speed. This corresponds to the critical flame initiation radius reported in previous theory [16] and experiments [27]. Successful ignition is achieved only when the ignition kernel can reach and propagate beyond the critical flame initiation radius [16,27]. In regime I, both S_b and K decrease as the ignition kernel propagates outwardly. Regimes II and III are the transition between ignition kernel propagation (regime I) and normal flame propagation (regime IV) [22,26]. In regime II, flame propagation is mainly driven by chemical reaction and transport rather than ignition energy deposited at the center. In regime II, S_b increases monotonically with R_f. The flame acceleration stops at point C, which corresponds to an overdriven flame with relatively high propagation speed. In regime III, the overdriven flame slows down and S_b decreases monotonically with R_f along curve CD. The existence of overdriven flame speed is very sensitive to the ignition energy. Increase in ignition energy from 1.85 mJ to 2.78 mJ (i.e., line #2–#4 in Fig. 2), the overdriven flame of regime III disappears. Regime IV corresponds to the normal flame propagation, during which the flame propagation speed is only affected by stretch rate. Figure 3 shows that in regime IV, S_b changes almost linearly with K. Therefore, regime IV is popular used to measure the unstretched laminar flame speed and Markstein length [23].

Unlike previous studies [22,26] in which only three regimes (corresponding to regimes I, II and IV here) were found, in this study the overdriven flame propagation regime (III) is identified for the first time. Though caused by different mechanisms, this overdriven flame propagation is similar to the overdriven detonation observed in direct detonation initiation [28]. Figure 2 shows that the overdriven flame regime disappears when the ignition energy is much larger than the MIE (i.e., $E = 2.78$ mJ, line #4 in Fig. 2b). Therefore, only three flame regimes, I, II and IV, appear when the ignition energy is not very close to the MIE. This could be the reason that only three regimes were found in [22,26].

Figure 4 shows the change of the heat release rate, Q, with the normalized temperature, θ. Here $\theta = (T - T_0)/(T_{ad} - T_0)$ with T_0 and T_{ad} being the unburned and adiabatic temperatures, respectively. θ can be used as the reaction progress variable for premixed flame. The CHEMIKIN-PREMIX results for unstretched adiabatic planar flame are shown together for comparison. Figure 4 indicates that in the overdriven flame propagation regime (III) and the normal flame propagation regime (IV), the profile of $Q(\theta)$ is nearly unaffected by stretch and very close to that of unstretched adiabatic planar flame. This fact helps to simplify flamelet modelling of certain type of turbulent premixed combustion [29]. However, Fig. 4 also indicates that in the ignition kernel propagation regime (I) and the unsteady flame transition regime (II), the $Q(\theta)$ profile changes significantly and is greatly different from that of unstretched adiabatic planar

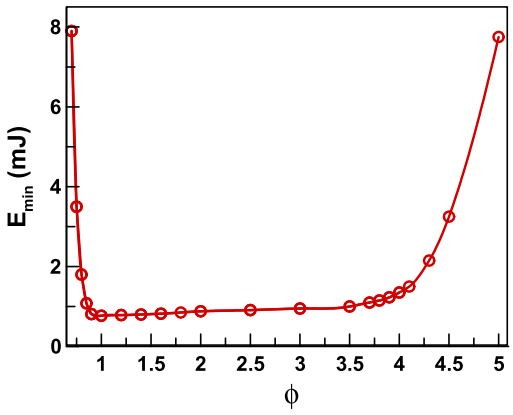

Fig. 5. Change of the minimum ignition energy with equivalence ratio for homogeneous $nC_{10}H_{22}$/air mixtures.

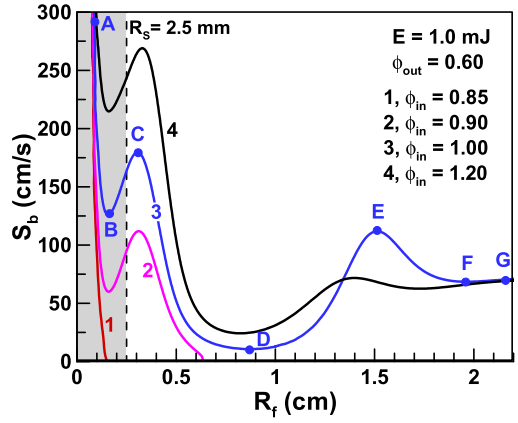

Fig. 6. Change of the flame propagation speed with flame radius for fuel-stratified $nC_{10}H_{22}$/air with different values of ϕ_{in} and fixed values of $\phi_{out} = 0.6$, $E = 1.0$ mJ and $R_S = 2.5$ mm.

flame. Therefore, special attention is required for flamelet modelling of turbulent combustion with ignition kernel development.

The above results are for homogeneous $nC_{10}H_{22}$/air with $\phi = 0.8$. Similar results are obtained for other values of equivalence ratio. Figure 5 summarizes the MIE for homogeneous $nC_{10}H_{22}$/air mixtures. With the increase of the equivalence ratio, the MIE first decreases rapidly from $E_{min} = 7.9$ mJ for $\phi = 0.7$ to $E_{min} = 0.81$mJ for$\phi = 0.9$; and then it approaches to a constant value for $0.9 < \phi < 3.5$. For lean $nC_{10}H_{22}$/air mixture, the effective Lewis number is above unity and it increases as the equivalence ratio decreases. Since the MIE increases greatly with the increase of Lewis number [16], leaner $nC_{10}H_{22}$/air mixture has much larger MIE. Figure 5 indicates that for fuel-lean n-decane/air mixture, the MIE is very sensitive to the equivalence ratio and that slight increase in ϕ can greatly reduce the MIE. Therefore, fuel stratification is expected to enhance ignition and reduce the MIE for fuel-lean n-decane/air mixture. This is investigated in the next subsection. For very rich $nC_{10}H_{22}$/air mixture, the effective Lewis number is below unity and it decreases as the equivalence ratio increases. Thereby the traditional U-shaped curve is obtained, which agrees qualitatively with experimental results [14,16,20,25]. However, it is difficult to achieve quantitative agreement in MIEs from simulation and experiments due to the simplified model used in simulation.

3.2. Fuel-stratified mixture

In this subsection, ignition and spherical flame propagation in fuel-stratified n-decane/air mixtures (i.e., $\phi_{in} \neq \phi_{out}$) are considered. As mentioned before, fuel stratification is characterized by three parameters, ϕ_{in}, ϕ_{out} and R_S. In the following, we fix two of these three parameters and assess the influence of the third parameter on ignition kernel propagation.

Figure 6 demonstrates the influence of inner equivalence ratio on ignition in fuel-stratified $nC_{10}H_{22}$/air mixture. The results for different values of ϕ_{in} and fixed values of $\phi_{out} = 0.6$, $E = 1.0$ mJ and $R_S = 2.5$ mm are presented. For $\phi_{in} = 0.85$ (line #1 in Fig. 6), flame propagation speed decreases quickly to zero and ignition fails. This is expected since the ignition energy of $E = 1.0$ mJ is smaller than the MIE of $E_{min} = 1.08$ mJ for homogeneous mixture with $\phi = 0.85$. For $\phi_{in} = 0.9$ (line #2 in Fig. 6), the ignition kernel can propagate beyond the stratification radius R_S since the ignition energy of $E = 1.0$ mJ is larger than the MIE of $E_{min} = 0.81$ mJ for homogeneous mixture with $\phi = 0.9$. However, after the flame reaches the outer zone with $\phi_{out} = 0.6$, its propagation speed eventually decreases to zero and ignition failure happens. When the inner equivalence ratio is further increased to $\phi_{in} = 1.0$ and 1.2 (lines #3 and #4 in Fig. 6), a self-sustained propagating spherical flame can be successfully initiated. It is noted that the ignition energy of $E = 1.0$ mJ is more than one-order smaller than the MIE for homogeneous mixture with $\phi = 0.6$. Therefore, Fig. 6 demonstrates that fuel stratification can greatly promote ignition for fuel-lean n-decane/air mixture.

Figure 6 indicates that there exist six distinct flame regimes for successful ignition with $\phi_{in} = 1.0$ (i.e., line #3 in Fig. 6): the ignition energy induced flame kernel propagation regime (I), the first unsteady flame transition regime (II), the fuel stratification induced flame kernel propagation regime (III), the second unsteady flame transition regime (IV), the overdriven flame propagation regime (V), and the normal flame propagation regime (VI). Regimes I to VI corresponds to AB, BC, CD, DE,

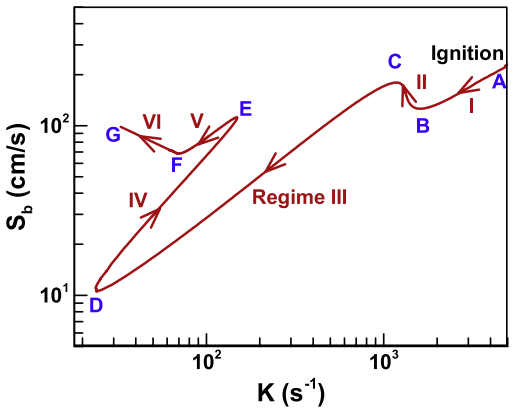

Fig. 7. Change of the flame propagation speed with stretch rate for fuel-stratified $nC_{10}H_{22}$/air with $\phi_{in} = 1.0$, $\phi_{out} = 0.6$, $E = 1.0$ mJ and $R_S = 2.5$ mm (same as line #3 in Fig. 6). The arrow indicates flame propagation direction (i.e., increase in flame radius).

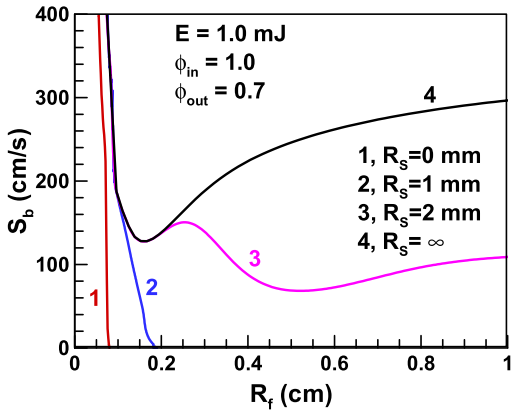

Fig. 9. Change of the flame propagation speed with flame radius for fuel-stratified $nC_{10}H_{22}$/air with different values of R_S and fixed values of $\phi_{in} = 1.0$, $\phi_{out} = 0.7$ and $E = 1.0$ mJ.

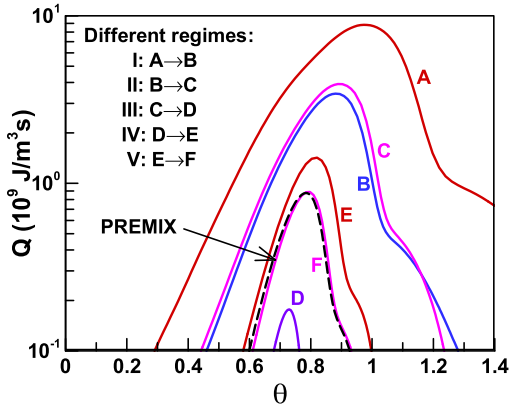

Fig. 8. Change of the heat release rate with normalized temperature for fuel-stratified $nC_{10}H_{22}$/air with $\phi_{in} = 1.0$, $\phi_{out} = 0.6$, $E = 1.0$ mJ and $R_S = 2.5$ mm. The dashed line corresponds to the PREMIX results for adiabatic planar flame with $\phi = 0.6$. Points A-F correspond to those in Figs. 6 and 7.

EF and FG in Fig. 6, respectively. These six regimes are more clearly demonstrated in Fig. 7, which plots the flame propagation speed as a function of stretch rate. Regimes I, IV, V and VI are similar to the four regimes of the homogeneous mixture discussed in Section 3.1. Regime I and III have the same trend in both S_b-R_f and S_b-K profiles. However, unlike regime I induced by ignition energy deposition, the ignition kernel propagation in Regime III is caused by fuel-stratification.

Similar to the homogeneous case (see Fig. 4), Fig. 8 shows the change of the heat release rate, Q, with the normalized temperature, θ, for ignition in fuel-stratified mixture with $\phi_{in} = 1.0$ and $\phi_{out} = 0.6$. The result for point G is not shown since it nearly overlaps with that for point F. In the normal flame propagation regime (VI, from F to G), the $Q(\theta)$ profile is very close to that of unstretched adiabatic planar flame. Therefore, the influence of stretch and fuel stratification can be neglected. However, for the first five regimes, I∼V, the $Q(\theta)$ profile changes significantly and is greatly different from PREMIX results (the dash line in Fig. 8). This is consistent with the conclusion in [30] that the change in equivalence ratio can affect greatly the heat release rate. Therefore, the influence of unsteady ignition and fuel stratification cannot be neglected in flamelet modeling of turbulent ignition process. However, it is challenging to deal with the unsteady ignition and fuel stratification in flamelet modelling. This deserves further study.

Stratified ignition depends on not only the inner equivalence ratio, ϕ_{in}, but also the stratification radius, R_S. Figure 9 plots the flame propagation speed as a function of flame radius for different values of R_S and fixed values of $\phi_{in} = 1.0$, $\phi_{out} = 0.7$ and $E = 1.0$ mJ. It is noted that $R_S = 0$ mm and $R_S = \infty$ correspond to homogeneous mixtures with $\phi = \phi_{out} = 0.7$ and $\phi = \phi_{in} = 1.0$, respectively. As expected, ignition failure happens to small stratification radius ($R_S = 0$ mm and $R_S = 1$ mm) while successful ignition occurs for large stratification radius ($R_S = 2$ mm and $R_S = \infty$). Therefore, for given values of ϕ_{in}, ϕ_{out}, and E, there is a critical stratification radius, beyond which successful ignition occurs.

In the present work, only simulations are conducted and there is no experimental validation. To our knowledge, the only experiment on ignition in stratified mixtures was reported in [5], in which the early evolution of ignition kernel was not captured. Therefore, no comparison between experiments and simulations is made in this work.

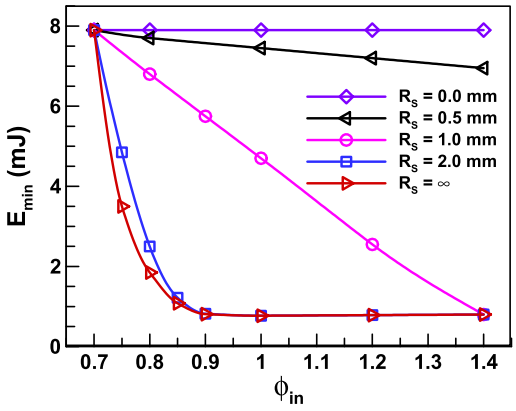

Fig. 10. The MIE as a function of inner equivalence ratio for fuel-stratified $nC_{10}H_{22}$/air mixtures with different values of R_S and fixed values of $\phi_{out} = 0.7$.

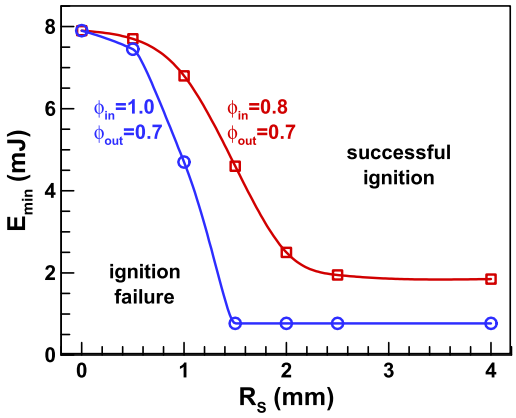

Fig. 11. The MIE as a function of stratification radius for fuel-stratified $nC_{10}H_{22}$/air mixtures with two different values of ϕ_{in} and fixed values of $\phi_{out} = 0.7$.

Certainly, experiments on fuel-stratified spark ignition deserve further study.

The above results indicate that fuel-stratification promotes ignition of lean $nC_{10}H_{22}$/air mixture and that successful ignition can be achieved by increasing the inner equivalence ratio and/or stratification radius. To quantify ignition promotion by fuel-stratification, we investigate the influence of inner equivalence ratio and stratification radius on the MIE. The MIEs for 36 sets of (ϕ_{in}, ϕ_{out} and R_S) are calculated. The results are summarized in Figs. 10 and 11.

Figure 10 depicts the change of the MIE, E_{min}, with inner equivalence ratio, ϕ_{in}. The results for different values of stratification radius are plotted together for comparison. The case of $R_S = \infty$ corresponds to the homogeneous mixture with $\phi = \phi_{in}$. Consequently, the results for $R_S = \infty$ in Fig. 10 are the same as those shown in Fig. 5 for homogeneous $nC_{10}H_{22}$/air. The case of $R_S = 0$ mm corresponds to the homogeneous mixture with $\phi = \phi_{out} = 0.7$. Therefore, the MIE has fixed value of $E_{min} = 7.9$ mJ for $\phi = 0.7$ and it is independent of ϕ_{in}. The results in Fig. 10 indicate how fuel-stratification affects the MIE of fuel-lean ($\phi = 0.7$) $nC_{10}H_{22}$/air mixture.

For small value of stratification radius, $R_S = 0.5$ mm, the ignition promotion due to fuel-stratification is not substantial: the largest reduction in MIE occurs to $\phi_{in} = 1.4$ and the MIE is 6.95 mJ (only 12% lower than 7.9 mJ). When the stratification radius is increased to $R_S = 1.0$ mm, the MIE is greatly reduced. The MIE decreases almost linearly with ϕ_{in} for $R_S = 0.5$ mm and $R_S = 1.0$ mm. When the stratification radius is further increased to $R_S = 2$ mm, the MIE is shown to decrease rapidly with the increase of ϕ_{in} and it approaches to a nearly constant value for $\phi_{in} \geq 0.9$. For $R_S = 2$ mm and $\phi_{in} = 0.9$, the MIE is $E_{min} = 0.82$ mJ, which is about one-order smaller than $E_{min} = 7.9$ mJ for the case without fuel-stratification and $\phi = 0.7$. Therefore, fuel-stratification with $R_S = 2$ mm can greatly enhance the ignition and reduce the MIE for fuel-lean ($\phi = 0.7$) $nC_{10}H_{22}$/air mixture. It is noticed that for the case of $R_S = 2$ mm, further increase of the inner equivalence ratio does not obviously reduce the MIE once $\phi_{in} \geq 0.9$. This indicates that for certain value of stratification radius, there is a minimum value of inner equivalence ratio for ignition enhancement beyond which there is no sensitivity. On the other hand, there should exist an optimum stratification radius for a given inner equivalence ratio. This fact is demonstrated by Fig. 11.

Figure 11 shows the change of the MIE with the stratification radius for fuel-stratified $nC_{10}H_{22}$/air with ($\phi_{in} = 0.8$, $\phi_{out} = 0.7$) and ($\phi_{in} = 1.0$, $\phi_{out} = 0.7$). Successful ignition is achieved for values of E and R_S above the curves in Fig. 11; otherwise ignition failure happens. With the increase of the stratification radius, the MIE decreases rapidly and it approaches to a nearly constant value at $R_S = 1.5$ mm for $\phi_{in} = 1.0$ and at $R_S = 2.5$ mm for $\phi_{in} = 0.8$. Further increase in stratification radius does not help to reduce the MIE. Therefore, there exists an optimum stratification radius for a given inner equivalence ratio. Similar to Fig. 9, Fig. 11 also shows that for given values of ϕ_{in}, ϕ_{out}, and E, there is a minimum value of stratification radius beyond which there is no sensitivity. Besides, Fig. 11 indicates that such stratification radius decreases as ϕ_{in} increases. Therefore, effective ignition enhancement can be achieved by choosing proper values of stratification radius and inner equivalence ratio.

4. Conclusions

Ignition and spherical flame kernel propagation in homogeneous and fuel-stratified n-decane/air

mixtures are studied by 1D simulation. The effects of fuel stratification on critical ignition condition and spherical flame kernel propagation are examined. The main conclusions are:

1. For fuel lean homogeneous n-decane/air mixture, the MIE is very sensitive to the equivalence ratio and slight increase in ϕ can greatly reduce the MIE. Therefore, fuel stratification is expected to enhance ignition and reduce the MIE for fuel-lean n-decane/air mixture. Besides, four distinct flame regimes are observed for the ignition kernel propagation, among which the overdriven flame propagation regime (III) is identified for the first time and it appears only when the ignition energy is slightly above the MIE.
2. For fuel-stratified n-decane/air mixture, both the ignition kernel propagation and the MIE are strongly affected by the inner equivalence ratio ϕ_{in} and stratification radius R_S. Six distinct flame regimes are observed for successful ignition in fuel-stratified mixture. The ignition kernel propagation can be induced by not only the ignition energy deposition but also the fuel-stratification. As shown in Figs. 10 and 11, for fuel-lean n-decane/ air mixture, fuel-stratification can greatly promote ignition kernel propagation and reduce the MIE. Effective ignition enhancement through fuel stratification can be achieved by choosing proper values of inner equivalence ratio and stratification radius. This indicates that fuel-stratified ignition can be used to achieve reliable ignition at ultra-lean conditions.

It is noted that the only one fuel, n-decane, is considered here. Nevertheless, similar results are obtained also for iso-octane, and the same conclusions are expected to hold for other large hydrocarbon fuels. In this study, the pre-mixture is static before ignition. As an extension of present work, the influence of flow and fuel-stratification coupling on ignition deserves further study.

Acknowledgments

This work was supported by National Natural Science Foundation of China (Nos. 91741126 and 91541204). We appreciate helpful discussion with Professor Yiguang Ju at Princeton University.

Supplementary materials

Supplementary material associated with this article can be found, in the online version, at doi:10.1016/j.proci.2018.05.087.

References

[1] A.C. Alkidas, *Energy Convers. Manage.* 48 (2007) 2751–2761.
[2] M. Aliramezani, I. Chitsaz, A.A. Mozafari, *Int. J. Hydrogen Energy* 38 (2013) 10640–10647.
[3] Z. Zheng, M. Yao, *Fuel* 88 (2009) 354–365.
[4] Y. Bai, Z. Wang, J. Wang, SAE Technical Paper 2010-01-0597, 2010.
[5] Y. Ra, *Laminar Flame Propagation in a Stratified Charge* Ph.D. thesis, Massachusetts Institute of Technology, 1999.
[6] A.P. Da Cruz, A. Dean, J. Grenda, *Proc. Combust. Inst.* 28 (2000) 1925–1932.
[7] T. Kang, D.C. Kyritsis, *Proc. Combust. Inst.* 31 (2007) 1075–1083.
[8] T. Kang, D. Kyritsis, *Combust. Theor. Model.* 13 (2009) 705–719.
[9] R. Zhou, S. Hochgreb, *Combust. Flame* 160 (2013) 1070–1082.
[10] S. Balusamy, A. Cessou, B. Lecordier, *Combust. Flame* 161 (2014) 427–437.
[11] J. Zhang, J. Abraham, *Combust. Flame* 163 (2016) 461–471.
[12] D. Patel, N. Chakraborty, *Combust. Theory Model.* 18 (2014) 627–651.
[13] D. Patel, N. Chakraborty, *Combust. Sci. Technol.* 188 (2016) 1904–1924.
[14] B. Lewis, G. Von Elbe, *Combustion, Flames and Explosions of Gases*, Academic Press, New York, 2012.
[15] B. Deshaies, G. Joulin, *Combust. Sci. Technol.* 37 (1984) 99–116.
[16] Z. Chen, M.P. Burke, Y. Ju, *Proc. Combust. Inst.* 33 (2011) 1219–1226.
[17] Z. Chen, M.P. Burke, Y. Ju, *Proc. Combust. Inst.* 32 (2009) 1253–1260.
[18] Z. Chen, *Combust. Flame* 157 (2010) 2267–2276.
[19] P. Dai, Z. Chen, *Combust. Flame* 162 (2015) 4183–4193.
[20] M. Chaos, A. Kazakov, Z. Zhao, F.L. Dryer, S.P. Zeppieri, in: Eastern States Fall Technical Meeting of the Combustion Institute, Orlando, FL, USA, 2005.
[21] M. Chaos, A. Kazakov, Z. Zhao, F.L. Dryer, *Int. J. Chem. Kinet.* 39 (2007) 399–414.
[22] H.H. Kim, S.H. Won, J. Santner, Z. Chen, Y. Ju, *Proc. Combust. Inst.* 34 (2013) 929–936.
[23] Z. Chen, *Combust. Flame* 162 (2015) 2442–2453.
[24] W. Zhang, Z. Chen, W. Kong, *Combust. Flame* 159 (2012) 151–160.
[25] T.M. Sloane, P.D. Ronney, *Combust. Sci. Technol.* 88 (1993) 1–13.
[26] J.S. Santner, S.H. Won, Y. Ju, *Proc. Combust. Inst.* 36 (2017) 1457–1465.
[27] A.P. Kelley, G. Jomaas, C.K. Law, *Combust. Flame* 156 (2009) 1006–1013.
[28] C. Qi, Z. Chen, *Proc. Combust. Inst.* 36 (2017) 2743–2751.
[29] D. Bradley, P. Gaskell, X. Gu, *Combust. Flame* 104 (1996) 176–198.
[30] K.R. Dinesh, H. Shalaby, K. Luo, J. van Oijen, D. Thévenin, *Int. J. Hydrogen Energy* 41 (2016) 18231–18249.